ISIJ International, Vol. 59 (2019), No. 8, pp. 1495–1505

Numerical Investigation of the Effect of Inert Components on the Shrinkage Phenomenon of Coke

Shohei MATSUO,[1)]* Yasuhiro SAITO,[2)] Yohsuke MATSUSHITA,[3)] Hideyuki AOKI,[3)] Hideyuki HAYASHIZAKI[3,4)] and Seiji NOMURA[4)]

1) Department of Chemical Engineering, Graduate School of Engineering, Tohoku University. Now at Nippon Steel & Sumitomo Metal Corporation, Technical Research & Development Bureau, 20-1 Shintomi, Futtsu, Chiba, 293-8511 Japan.
2) Department of Applied Chemistry, Kyushu Institute of Technology, 1-1 Sensui-cho, Tobata-ku, Kitakyushu, Fukuoka, 804-3301 Japan.
3) Department of Chemical Engineering, Graduate School of Engineering, Tohoku University, 6-6-07 Aoba, Aramaki, Aoba-ku, Sendai, Miyagi, 980-8579 Japan.
4) Nippon Steel & Sumitomo Metal Corporation, Technical Research & Development Bureau, 20-1 Shintomi, Futtsu, Chiba, 293-8511 Japan.

(*Received on December 20, 2018; accepted on April 3, 2019*)

The effect of inert components in coke on the shrinkage ratio of coke was numerically investigated. The carbonization process of semi-coke was simulated by using the finite element method. Coke models with a coke matrix, pores, cracks, and/or inert components were used. The numerical results using a coke model composed of a coke matrix and pores indicated that pores did not affect the shrinkage behavior of semi-coke. In addition, cracks did not affect the shrinkage behavior. On the other hand, from a numerical simulation using a coke model with inert components, the addition of inert components decreased the shrinkage ratio of coke. When the inert components were added, the elastic modulus of the inert components, viscosity of the matrix of semi-coke, and size of the inert components affected the shrinkage ratio. Furthermore, cracks extending from the inert component drastically decreased the shrinkage ratio of coke because the thermal stress around the interface between the matrix and inert components opened the crack.

KEY WORDS: coke; shrinkage ratio; inert component; thermal stress analysis; coke size.

1. Introduction

Metallurgical coke plays a role in sustaining the flow passages of reaction gases and melted iron in a blast furnace. Since small coke particles fill voids in the blast furnace and inhibit the flow of gas and liquid, the size of the coke is one of the important qualities.[1)] The shrinkage ratio of coal affects the size of coke, and the coke size becomes smaller as the shrinkage ratio of coal increases.[2–4)] This is because large thermal stress is developed and many cracks are generated during the carbonization process when coal with a large shrinkage ratio is used.[3–5)] Hence, when the factor that determines the amount of contraction in coals during carbonization is clarified, the size of coke can be controlled.

Some studies on the shrinkage behavior of coal during carbonization have been carried out, and it was shown that the properties of coal significantly affected the shrinkage ratio of coke.[6–11)] One of the important properties of coal that determines the shrinkage ratio of coke is the amount of volatile matter (VM). This is because a larger amount of VM released from the coke decreases the more weight of coke, and it was reported that coal with a larger amount of VM contracted more.[8,9)] Regarding another coal property that affects the shrinkage of coke, Iwamoto *et al.*[11)] focused on the crystal and chemical structure of coals and reported that coke with higher carbon aromaticity at high temperature showed a higher shrinkage ratio. Alvarez *et al.*[10)] reported that the softening properties of coal affect the shrinkage ratio of coke, and that coals with a wide range of softening temperatures and lower viscosities had a higher shrinkage ratio of coke. However, in the industrial process, it is difficult to control the shrinkage ratio of coke with different types of coals because it is required to select coals by considering the strength and swelling pressure. Thus, the addition of inert materials is an effective way to control the size of coke. Fukada *et al.*[12)] showed that the addition of inert material such as coke breeze and anthracite reduced the amount of contraction of coke and increased the size of coke. In addition, Fukada *et al.* concluded that microcracks affected the shrinkage ratio of coke because many microcracks were generated in coke with an inert material. Thus, it is important to clarify the role of inert components in the shrinkage behavior of coke during carbonization. Although the effect of inert materials on the stress of the coke matrix and the strength of coke were examined in previous studies,[13–17)]

* Corresponding author: E-mail: matsuo@dc.tohoku.ac.jp
DOI: https://doi.org/10.2355/isijinternational.ISIJINT-2018-817

little is known about the effect on the contraction behavior.

To establish a technique for increasing the coke size, it is important to clarify the effect of inert materials in coke on its shrinkage behavior. The shrinkage of coke during carbonization is caused by thermal stress. Thus, understanding the distribution of the thermal stress developed in the coke is required in order to investigate the mechanism whereby inert components in the microstructure inhibit the shrinkage of coke. However, because the experimental measurement of thermal stress is difficult, a theoretical investigation is a more effective approach. Kubota *et al.*[13] estimated the thermal stress around an inert component based on the elastostatics and indicated that a high thermal stress developed around the inert component during the carbonization of coke. However, the researchers did not focus on the deformation of the inert component and the coke matrix, and did not discuss the effect of inert materials on the shrinkage. In addition, the researchers assumed that the shape of the inert component was a circle in a two-dimensional structure and that the body of the matrix was elastic. However, in general, the shape of an actual inert component is not a sphere, and the matrix shows viscous behavior during the shrinkage of semi-coke undergoing carbonization.[18,19] Thus, a quantitative investigation based on a simplified theoretical formula with many assumptions was insufficient, and a method that considers the shape of the inert components and the viscosity of the materials is desired. In the present study, we focus on a numerical analysis using the finite element method (FEM). FEM is a powerful tool to predict the stress distribution and the deformation behavior in the material. Recently, some stress analyses of coke using FEM were reported,[20–25] and most of these studies focused on the relationship between the structure of the pores and the stress concentration sites.[20–23] On the other hand, Ueoka *et al.*[24] performed a thermal stress analysis on coke models with circular inert components arranged randomly, and indicated that the arrangement of the inert components affected the maximum value of the thermal stress. Sato *et al.*[25] analyzed the thermal stress in coke during carbonization, and reported that the stress distribution and deformation behaviors of a coke model that was assumed to be a visco-elastic body differed from models with an elastic body. However, these analyses examined the thermal stress in coke and the fracture phenomena of coke, and did not focus on the shrinkage behavior of the coke during carbonization.

In the present study, we performed thermal stress analyses on the microstructure of coke with inert materials using FEM in order to clarify the effect of inert materials on the shrinkage behavior of coke. Furthermore, to understand the effect of the inert materials, the effect of a crack and a pore on the shrinkage of coke was also investigated. Moreover, we performed numerical analyses considering the viscosity of the matrix, and examined the effect of the viscosity of the shrinkage of coke.

2. Numerical Analysis

2.1. Analytical Objects and Boundary Conditions

The analytical object used was semi-coke in the shape of a cube with a side length of 30 mm consisting of a matrix, cracks, pores, and/or inert components. This is shown in **Fig. 1**. Since the geometry can be assumed to be symmetric, one-eighth of a domain was analyzed by using symmetric boundary conditions. In the present study, to represent a crack, a free boundary condition was adopted as a boundary condition, and nodes located at the bottom of the domain were unconstrained, as shown in Fig. 1(b). Thus, a crack was treated as a surface of the material without external forces. The coke model was assumed to have pores or inert components of 12.5% by volume, and the shape was a cube of 7.5 mm in side length, as shown in Fig. 1(c-1). To investigate the effect of the size of the inert component on the shrinkage behavior, 27 cubes of inert components with side lengths of 2.5 mm were arranged in the coke model, as indicated in Fig. 1(c-2). Note that the volume fractions of the inert components in the coke model shown in Figs. 1(c-1) and 1(c-2) were equal. Figure 1(d) shows an analytical object with an inert component and one crack. Kubota *et al.*[13] reported that cracks were generated around an inert component with a low shrinkage ratio. In the present study, a crack with a width of 3.75 mm on the *x*-*y* plane or *x*-*y*, *y*-*z*, and *z*-*x* planes was arranged in the analytical object to reproduce the crack generated around the inert component. The body of the semi-coke matrix was assumed to be elastic or visco-elastic. The elastic modulus and Poisson's ratio of the matrix were set to 1 GPa and 0.3, respectively. Those of the pore were 10^{-4} GPa and 0, respectively. A Maxwell model was applied to the visco-elastic coke matrix. Since a previous study reported that the relaxation time of semi-coke at a temperature of 650°C was approximately 60 s,[19] the relaxation time of the coke matrix in the coke model was assumed to be 60 s at temperatures of 400–700°C. In this case, the viscosity coefficient was 60 GPa·s because a Maxwell model was used. In addition, to examine the effect of the viscosity of the semi-coke, numerical analyses with matrix relaxation times of 6 and 600 s were performed. By referring to the experimental results of Nomura *et al.*,[2] the linear contraction coefficient shown in **Fig. 2** was prescribed for the semi-coke matrix in order to assume coal with a large shrinkage ratio. Note that the shrinkage ratio of coke at a temperature of 1 000°C was 17.50%. The coke model was heated from 450°C to 1 000°C at a heating rate of 3 K/min without considering the temperature distribution in the computational domain. The time increment was set to 30 s. The shrinkage ratio of the coke model, α, was quantitively evaluated from the following equation:

$$\alpha = 1 - \sqrt[3]{\frac{\left(\text{Total volume of the analytical object after shrinkage}\right)}{\left(\text{Initial total volume of the analytical objcet}\right)}}, \quad \ldots\ldots (1)$$

where the ratio was used to quantitatively evaluate the shrinkage behavior of coke. In the present study, to investigate the effect of the elastic modulus of an inert component on the shrinkage behavior, the elastic modulus of the inert component was set to 1, 3, and 10 GPa. The elastic modulus of the inert component was higher than that of the matrix because the elastic modulus of inert components are higher than those of active ones, as measured by Ogata *et al.*[26] using the nano-indentation method. Further, the inert component was assumed to be an unshrinkable material in

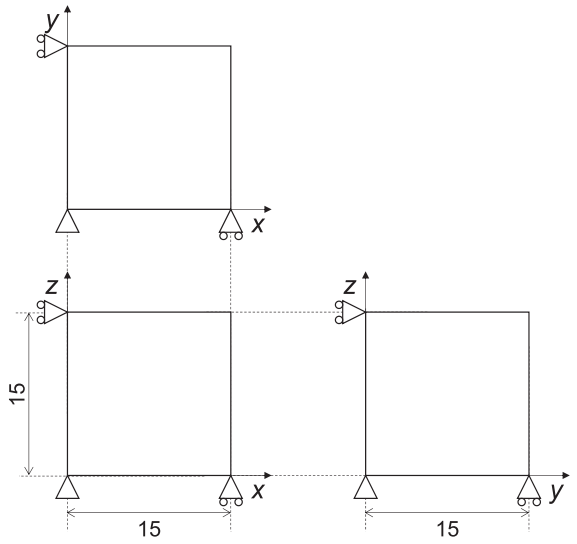

(a) Coke model with only coke matrix.

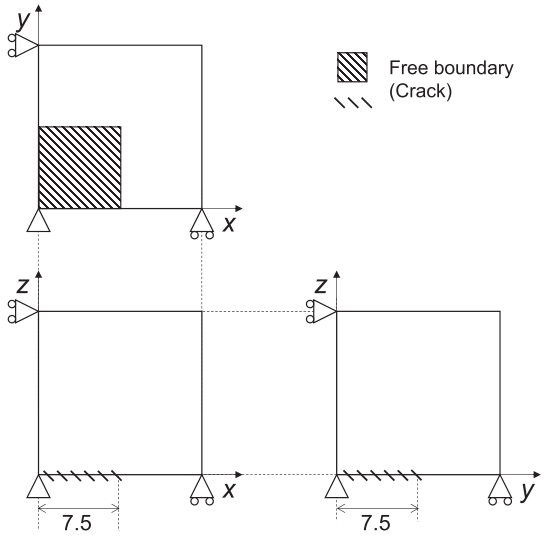

(b) Coke model with coke matrix and one crack.

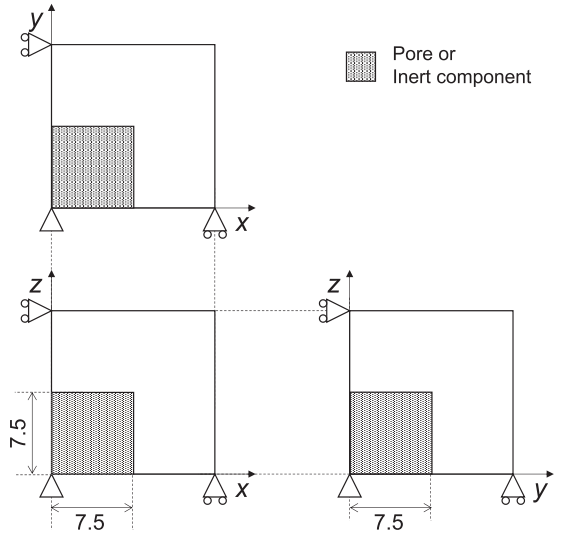

(c-1) Coke model with coke matrix and a pore or large inert component.

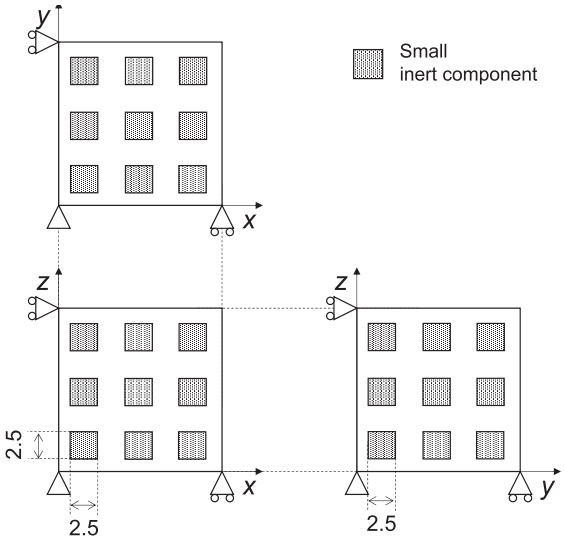

(c-2) Coke model with coke matrix and 27 small inert components.

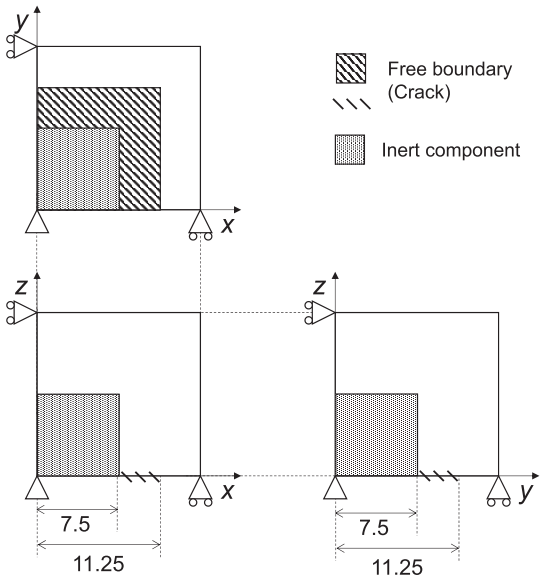

(d-1) Coke model with coke matrix, one crack, and an inert component.

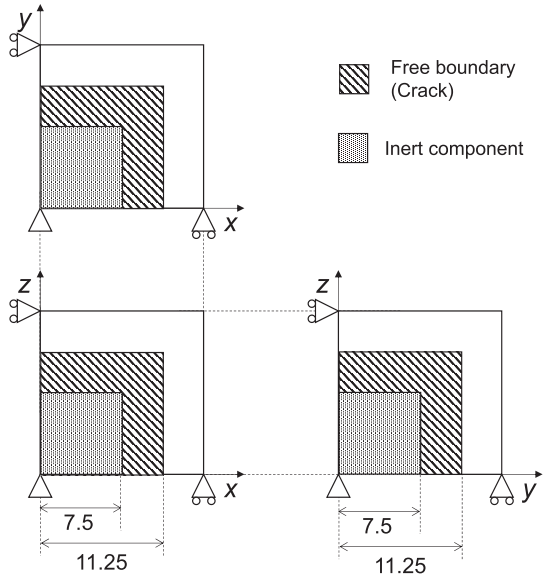

(d-2) Coke model with coke matrix, three cracks, and an inert component.

Fig. 1. Analytical objects.

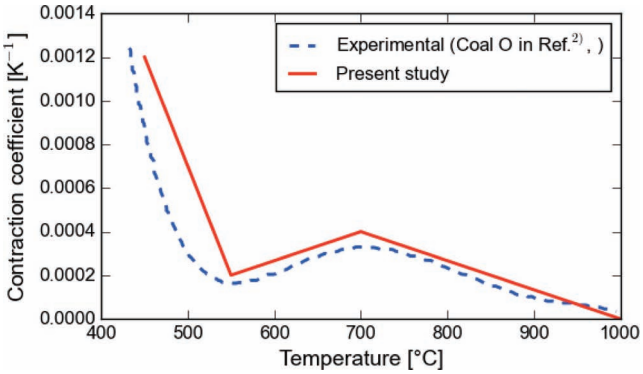

Fig. 2. Temperature-dependent contraction coefficient. (Online version in color.)

Table 1. Numerical conditions for coke models with inert components.

Number of inert components [num.]	1 or 27
Elastic modulus of inert component [GPa]	1, 3, or 10
Relaxation time of coke matrix [s]	6, 60, 600, or ∞
Number of cracks [num.]	0, 1, or 3

Here, when the number of cracks was 1, the crack was placed on the *x*-*y* plane. When the number of cracks was 3, the cracks were placed on the *x*-*y*, *y*-*z*, and *z*-*x* planes.

this study. Thus, the estimated value of the shrinkage ratio of the coke model, α_{estimate}, has no interaction between the matrix and inert component. The values for the coke models shown in Figs. 1(c-1), 1(c-2), and 1(d) were 14.90% at a temperature of 1 000°C. Moreover, it was assumed that the inert component was not viscous. In summary, we carried out numerical simulations for 26 coke models with inert components, as listed in **Table 1**.

2.2. Thermal Stress Analysis with Finite Element Method

The thermal stress in the shrinkage of semi-coke was numerically analyzed using the finite element method. Sato *et al.*[25] described the finite element formulations for two-dimensional visco-elastic material. In the present study, we used three-dimensional finite element formulations based on a theory described by Zienkiewicz *et al.*[27] When the temperature increases from T_n to T_{n+1}, the increment of the thermal stress, $\Delta\varepsilon^{th}$, is expressed as follows:

$$\Delta\varepsilon^{th} = \int_{T_n}^{T_{n+1}} \alpha(T)\,\mathrm{d}T, \quad \text{..... (2)}$$

where α is a contraction coefficient that depends on the temperature. In general, thermal stress contributes to isotropic deformation. Thus, an increment of the nodal force vector attributed to the thermal stress, $\Delta\mathbf{f}^{th}$, is obtained as follows:

$$\Delta\mathbf{f}^{th} = \int_{\Omega} \mathbf{B}^{\mathrm{T}}\mathbf{D}\Delta\varepsilon^{th}\mathbf{m}\mathrm{d}\Omega, \quad \text{..... (3)}$$

where **B** represents the B matrix, and **D** represents the elasticity matrix, respectively. Matrix **m** has the following components:

$$\mathbf{m}^{\mathrm{T}} = [1,1,1,0,0,0]. \quad \text{..... (4)}$$

The softening of coal was expressed with a Maxwell model. In general, viscous stress affects only the deviatoric direction. The deviatoric elastic strain, $\boldsymbol{\varepsilon}_d^e$, is calculated by the following equation:

$$\boldsymbol{\varepsilon}_{d,n+1}^{e} = \exp\left[-\frac{\Delta t}{\lambda}\right]\boldsymbol{\varepsilon}_{d,n}^{e} + \frac{\lambda}{\Delta t}\left(1-\exp\left[-\frac{\Delta t}{\lambda}\right]\right)\left(\boldsymbol{\varepsilon}_{d,n+1}-\boldsymbol{\varepsilon}_{d,n}\right), \quad \text{..... (5)}$$

where Δt is the time increment, and λ is the relaxation time. Thus, the tangential stiffness matrix $\mathbf{D}_{\mathrm{T}}$, which is used to linearize the finite element equations, is written as follows:

$$\mathbf{D}_{\mathrm{T}}|_{n+1} = \left.\frac{\partial\boldsymbol{\sigma}}{\partial\boldsymbol{\varepsilon}}\right|_{\varepsilon_{n+1}} = K\mathbf{m}\mathbf{m}^{\mathrm{T}} + 2\mathrm{G}\frac{\lambda}{\Delta t}\left(1-\exp\left[-\frac{\Delta t}{\lambda}\right]\right)\left(\mathbf{I}-\frac{1}{3}\mathbf{m}\mathbf{m}^{\mathrm{T}}\right), \quad \text{.... (6)}$$

where K is the bulk modulus, G is the shear modulus, and **I** is the identity matrix. From the above equations, an incremental finite element equation for the thermal stress and visco-elastic analyses is expressed as

$$\left(\int_{\Omega}\mathbf{B}^{\mathrm{T}}\mathbf{D}_{\mathrm{T}}|_{n+1}\,\mathbf{B}\mathrm{d}\Omega\right)\Delta\mathbf{d} = \Delta\mathbf{f}^{th} - \int_{\Omega}2G\left(\exp\left[-\frac{\Delta t}{\lambda}\right]-1\right)\mathbf{B}^{\mathrm{T}}\boldsymbol{\varepsilon}_{d,n}^{e}\mathrm{d}\Omega. \quad \text{..... (7)}$$

3. Results and Discussion

3.1. Effect of Existence of a Crack and Pore in Semi-coke on Shrinkage Ratio

To investigate the effect of the existence of a crack and a pore in semi-coke on the shrinkage ratio, shrinkage ratios in coke models with the semi-coke matrix only, with the semi-coke matrix and a crack, and with the semi-coke matrix and a pore are shown in **Fig. 3**. The volume of the coke model with only the coke matrix after shrinkage was 1 895 mm^3. The shrinkage ratio calculated with Eq. (1) was 17.50% and corresponded to the prescribed value. **Figure 4** displays the deformed coke and von Mises stress distribution after shrinkage. The model with only the coke matrix shrank isotropically, and the von Mises stress did not occur. These results ensured that our shrinkage analysis with FEM was fully verified.

The results of the coke models with the matrix only [in Fig. 1(a)] and with the matrix and a crack [in Fig. 1(b)] are compared. The shrinkage ratio of the coke model with the matrix and crack perfectly agreed with that with the matrix only. Focusing on the stress distribution, deviatoric stress was not developed in the coke model with the matrix and a crack, as was the case in that with the matrix only. In general, stress concentrates at the crack tip in a material under loading conditions. On the other hand, in the present analysis, since the elastic modulus and contraction coefficient of the matrix were uniform, the matrix was only forced isotropically. Thus, since a crack treated as a free boundary condition shrank isotropically, little deviatoric stress should develop. Furthermore, as is the case in the coke model with the matrix and a crack, the shrinkage ratio of the model with a pore corresponded to that with the matrix only, and the von Mises stress did not occur. This is because the pore could also deform like the crack, and shrink isotropically.

These results indicate that the pore and crack did not affect the shrinkage behavior of coke directly when only a pore and a crack were arranged in the coke model.

3.2. Effect of Existence of Inert Component on Shrinkage Ratio of Coke

To investigate the effect of the existence of an inert component on the shrinkage ratio of coke, volumetric changes in the entire semi-coke (*i.e.*, the matrix and an inert component that was assumed to be an elastic body) are shown in **Fig. 5**. The elastic modulus of the inert component affected the shrinkage behavior. The shrinkage ratio of coke could not be estimated easily when inert components were added because the contraction coefficients of the matrix in each model were the same. **Figure 6** shows the shrinkage ratio of the entire semi-coke which consisted of the matrix and the inert component. With the assumption that the coke matrix body was elastic, the shrinkage ratio was large when the elastic modulus of the inert component was 1 GPa. On the other hand, the shrinkage ratio was small when the elastic modulus was 3 or 10 GPa. Since the shrinkage ratio was

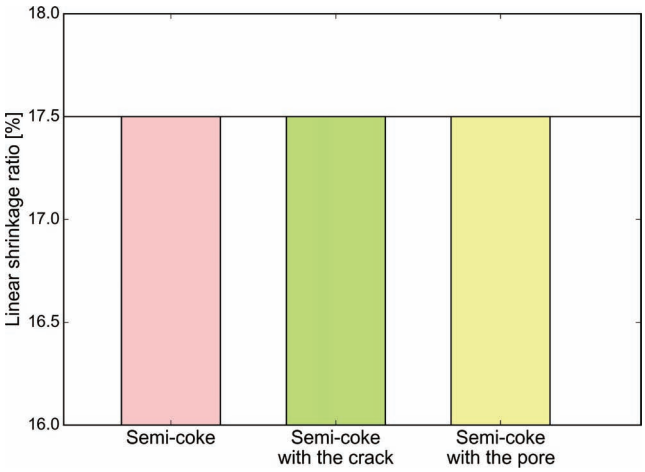

Fig. 3. Shrinkage ratios of coke models with only coke matrix, coke matrix and a crack, and coke matrix and a pore. Coke matrix is assumed to be elastic. Solid line is estimated value of coke model consisting of only coke matrix. (Online version in color.)

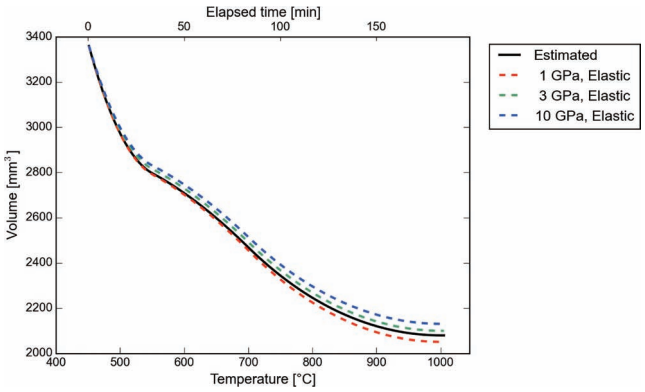

Fig. 5. Effect of elastic modulus of inert component on volumes of coke model with coke matrix and large inert component. Coke matrix is assumed to be elastic. (Online version in color.)

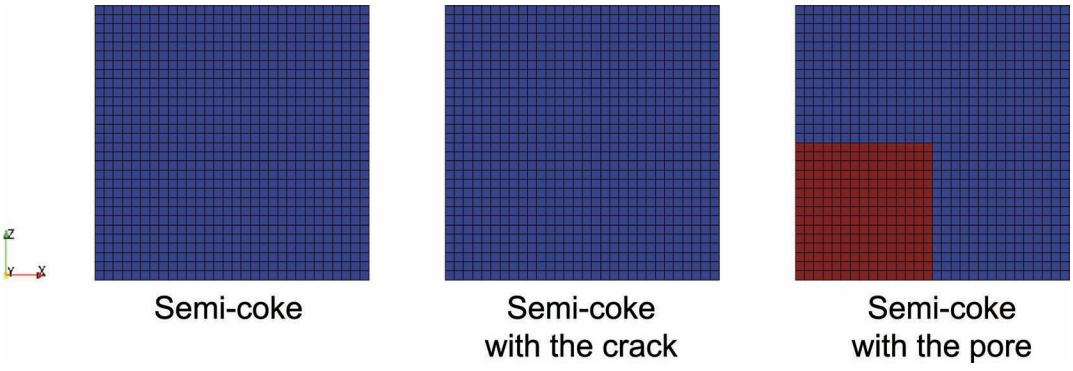

(i) Material arrangement. Blue-colored parts are coke matrices, and red-colored parts represent pores in computational domain.

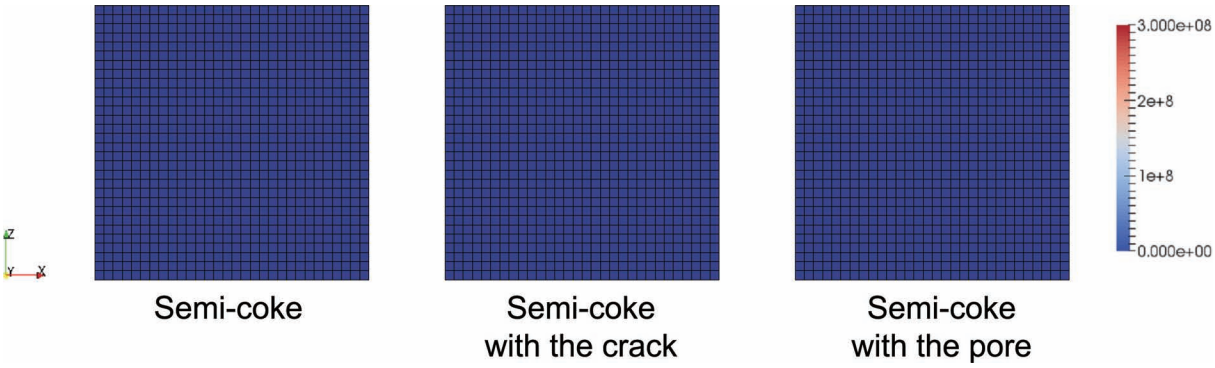

(ii) von Mises stress distribution.

Fig. 4. Deformed coke and von Mises stress distribution in direction of $y = 0$ mm and temperature of 1 000°C. Coke matrix is assumed to be elastic. (Online version in color.)

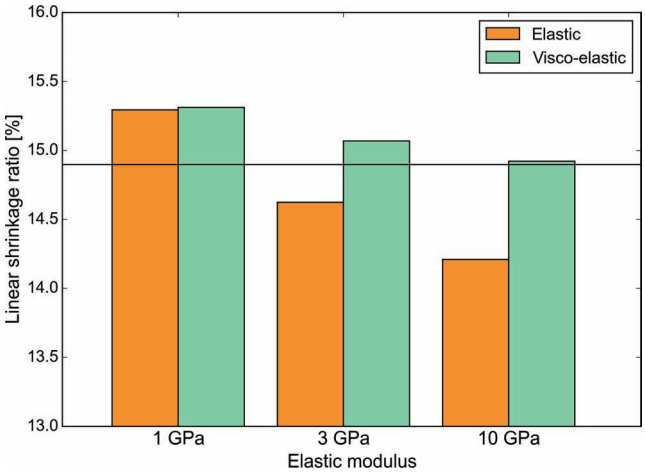

Fig. 6. Effect of elastic modulus of inert component on shrinkage ratios of coke model with coke matrix and large inert component. Coke matrix is assumed to be elastic or visco-elastic. Line represents estimated value of coke model with coke matrix and 12.5% of inert component. (Online version in color.)

the smallest for an elastic modulus of 10 GPa, the shrinkage ratio of coke should decrease with an increase in the elastic modulus of the inert component. To discuss the reason for the above, the deformation behavior and stress distribution of coke after the contraction are displayed in **Fig. 7**. In Fig. 7(a), the body of the matrix was assumed to be elastic, and the von Mises stress occurred in the interface between the inert component and matrix. This corresponds to previous studies by Kubota *et al.*[13] and Ueoka *et al.*[24] in which thermal stress developed around the inert component because of the difference in the contraction between the inert component and the matrix. When the elastic modulus of the inert component was 1 GPa, the inert component was deformed. This deformation should be attributed to the shrinkage force caused by the contraction of the matrix. The reason for the high shrinkage ratio when the elastic modulus of the inert component was the same as that of the matrix (in Fig. 6) should be the shrinkage of the inert component. On the other hand, when the elastic modulus was 3 or 10 GPa, the deformation of the inert component was small. The reason for the low shrinkage ratio of the entire coke when the elastic modulus of the inert component was large should be that the deformation of the matrix was inhibited by the inert component. Focusing on the case where the matrix body of semi-coke was assumed to be visco-elastic, the shrinkage ratio of coke was large (as shown in Fig. 6), the von Mises stress was small, and the deformation of the inert component was small [as displayed in Fig. 7(b)]. This is because the apparent elastic modulus of the matrix decreased owing to viscosity, and the elastic modulus of the inert component increased relatively. In addition, the matrix was significantly deformed around the interface between the inert component and the matrix, and the deformation should be caused by the thermal stress. Sato *et al.*[25] numerically showed that the deformation volume of semi-coke of which the matrix body was assumed to be elastic was different from that of visco-elastic matrix body owing to the thermal stress. Although, the results in this study cannot be directly compared to those in Sato *et al.* because of differences in the sizes of the analytical objects, it is indicated that the viscosity affects the shrinkage behavior of coke. Therefore, when considering the viscosity, an increase in the shrinkage ratio of coke should be caused by the deformation of the softening matrix in the shrinkable direction owing to the stress developed at the interface between the matrix and the inert component. To investigate the shrinkage behavior during the heating process, the difference between contraction coefficient α and estimated contraction coefficient $\alpha_{estimated}$ (*i.e.*, $\Delta\alpha$) is shown in **Fig. 8**. $\Delta\alpha$ increased and decreased monotonically with an increase in the temperature when the matrix body was assumed to be elastic. Meanwhile, when the matrix body was assumed to be visco-elastic, $\Delta\alpha$ increased with the shrinking of the matrix as the viscosity increased to 700°C. However, over 700°C, $\Delta\alpha$ increased when the elastic modulus of the inert component was assumed to be 1 GPa, and decreased when the elastic modulus was 3 and 10 GPa. These tendencies over 700°C were similar to those when the matrix was assumed to be an elastic body. This is because our numerical simulation assumed that the behavior of the matrix was visco-elastic below 700°C and elastic above 700°C.

To examine the effect of the viscosity coefficient on the shrinkage behavior, $\Delta\alpha$ with different relaxation times is shown in **Fig. 9**. The elastic modulus of the inert component was set to 3 GPa in each case. The shrinkage ratio increased with a decrease in the relaxation time of the matrix. This is because the viscosity was lower for a shorter relaxation time, and the matrix can be deformed easily. Alvarez *et al.*[10] reported that the shrinkage ratio of coke produced with coal with a wide softening temperature range and low viscosity was large, and our numerical result was consistent with the experimental one. Focusing on the result at a relaxation time of 600 s, $\Delta\alpha$ decreased in the early stage of the shrinkage. On the other hand, for relaxation times of 6 and 60 s, $\Delta\alpha$ decreased little. These results showed that the relaxation time significantly affected $\Delta\alpha$ in the early stage of the shrinkage. This should be because the stress was not relaxed sufficiently when the shrinkage rate was high in the early stage of the shrinkage and the relaxation time was long. Therefore, it is suggested that the shrinkage ratio of coke became larger for semi-coke with a lower viscosity, and that the viscosity significantly affected the shrinkage ratio in the early stage of the shrinkage.

3.3. Effect of Size of Inert Component on Shrinkage Ratio

To investigate the effect of the size of the inert component on the shrinkage ratio, the shrinkage ratio of the coke model with 27 small inert components is shown in **Fig. 10**. When the elastic modulus of the inert component was 1 GPa, the difference in the shrinkage ratio of the coke model with small inert components and that with large components was slight. By contrast, when the elastic moduli of the inert components were 3 and 10 GPa (*i.e.*, the elastic modulus of the inert components was larger than that of the matrix), the shrinkage ratio of coke decreased. The reason for the decrease of the shrinkage ratio should be that the interface area between the inert components and the matrix increased, and the inhibition effect of the inert components on the contraction was large when the small inert components were

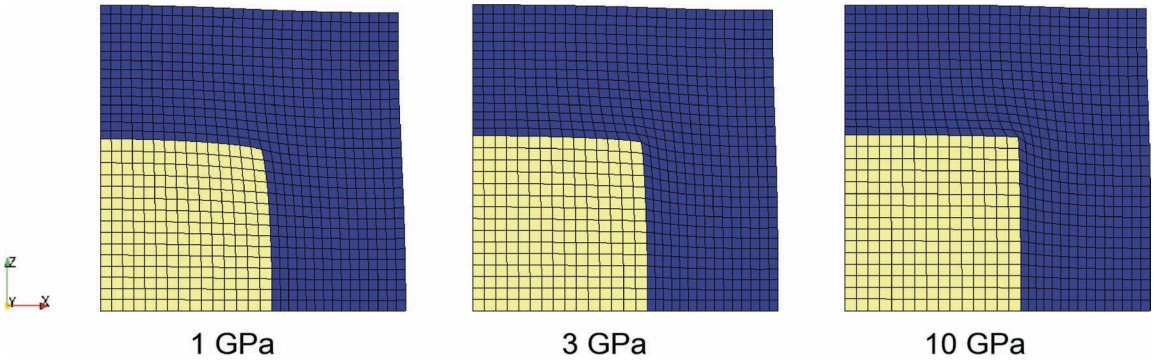

(a-1) Material arrangement. Blue-colored parts are coke matrices, and yellow-colored parts represent inert components in computational domain. (Matrix is assumed to be elastic.)

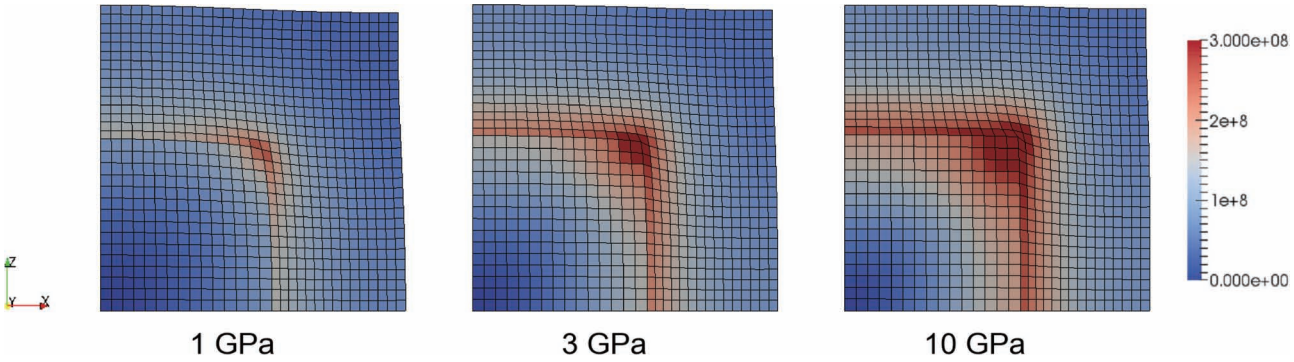

(a-2) von Mises stress distribution. (Matrix is assumed to be elastic.)

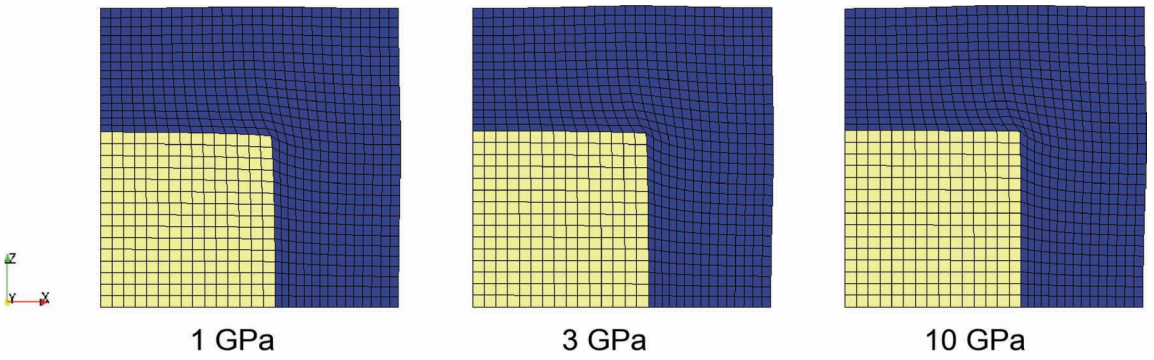

(b-1) Material arrangement. Blue-colored parts are coke matrices, and yellow-colored parts represent inert components in computational domain. (Matrix is assumed to be visco-elastic.)

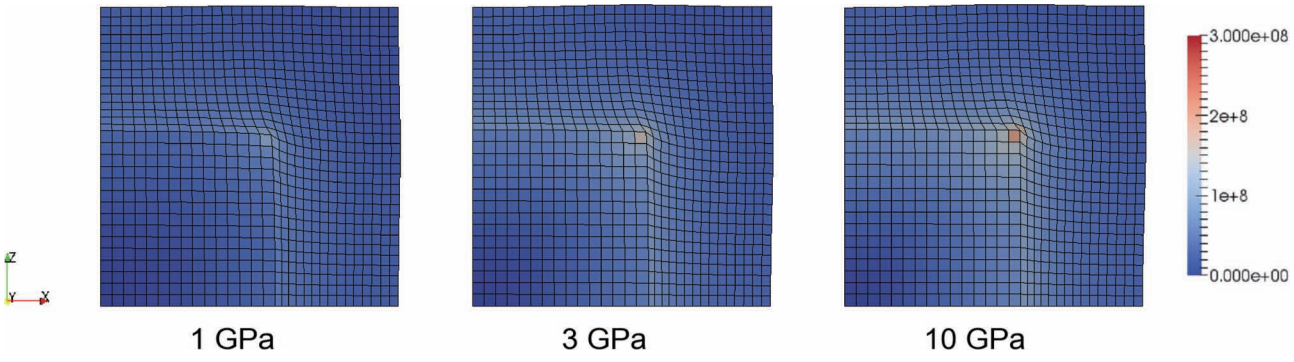

(b-2) von Mises stress distribution. (Matrix is assumed to be visco-elastic.)

Fig. 7. Deformed coke and von Mises stress distribution of coke model with coke matrix and large inert component in direction of y = 0 mm and temperature of 1 000°C with various elastic moduli of inert component. (Online version in color.)

arranged. However, the effect of the size of the inert component on the shrinkage ratio was relatively smaller than that of the elastic modulus of the inert component and the viscosity of the matrix. To discuss this reason, the deformation behavior of coke and the stress distribution in the coke model with small inert components as displayed in **Fig. 11**

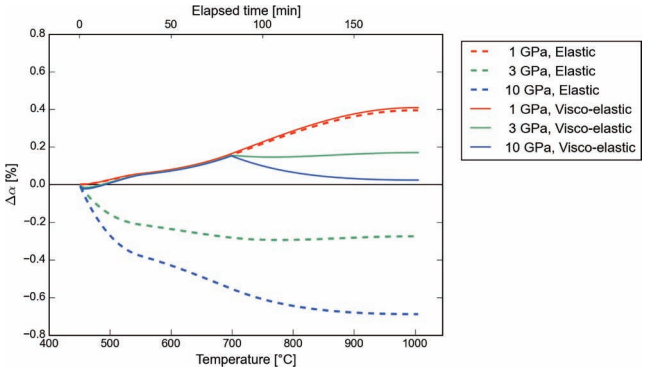

Fig. 8. Differences between numerical shrinkage ratio and estimated shrinkage ratio for various elastic moduli of inert component. (Online version in color.)

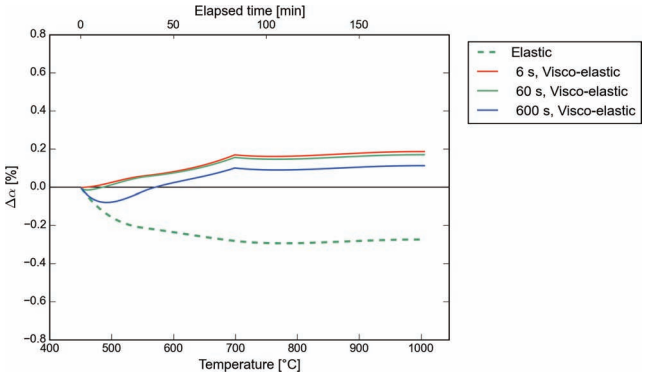

Fig. 9. Differences between numerical shrinkage ratio and estimated shrinkage ratio with various conditions of viscosity (elastic modulus of inert component is 3 GPa). (Online version in color.)

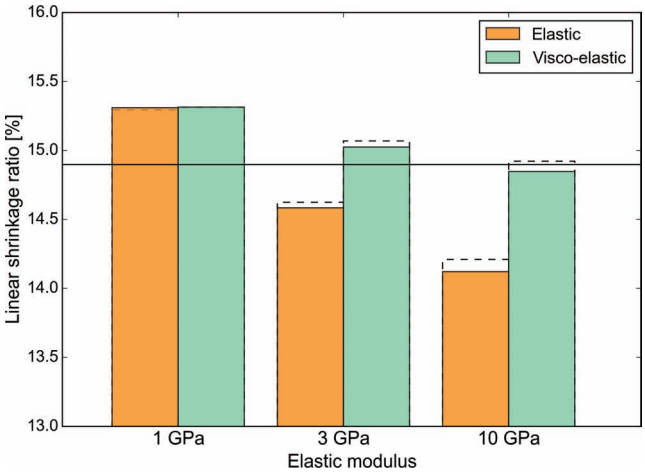

Fig. 10. Effect of elastic modulus of inert component on shrinkage ratios of coke model with coke matrix and small inert components. Coke matrix is assumed to be elastic or visco-elastic. Line represents estimated value of coke model with coke matrix and 12.5% of inert component. Broken line represents result of Fig. 6. (Online version in color.)

are investigated. Focusing on the deformation behavior of the matrix in the vicinity of the inert components, anisotropic deformation was observed around the inert components as with the coke model with the large inert component in each condition. However, in each condition, the deformation volume of the matrix around the inert components

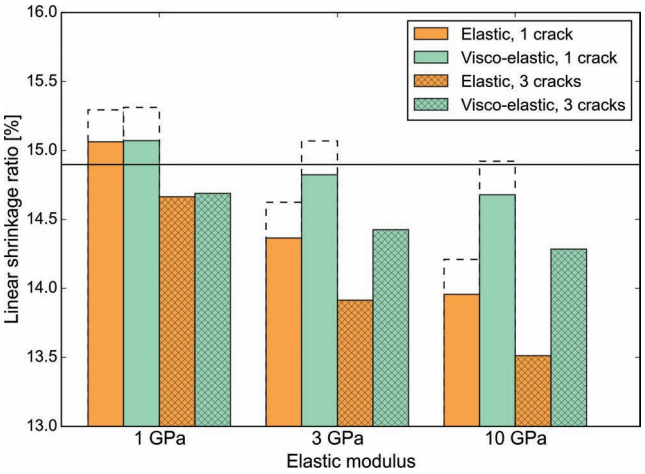

Fig. 12. Effect of elastic modulus of inert component on shrinkage ratios of coke model with coke matrix, inert component, and one or three cracks. Coke matrix is assumed to be elastic or visco-elastic. Line represents estimated value of coke model with coke matrix and 12.5% of inert component. Broken line represents result of Fig. 6. (Online version in color.)

was smaller with the small inert components than with the large inert component. Further, the von Mises stress in the model decreased because of the decrease in the size of the inert component. Therefore, the decrease in the deformation volume of the coke matrix is thought to be caused by the decrease in the thermal stress. From the above discussion, when the size of the inert components was small, although the shrinkage ratio of the coke decreased because of the large surface area of the inert components, the effect of the size of the inert component on the shrinkage ratio was small; this is because of the decrease in the thermal stress developed in the interface between the inert component and the matrix.

3.4. Effect of Cracks Generated around Inert Component on Shrinkage Ratio

To investigate the effect of cracks generated around the inert component on the shrinkage ratio, **Fig. 12** shows the shrinkage ratio of the coke model with an inert component and crack(s). In each case with the crack arrangement, the shrinkage ratio decreased. To discuss the reason for the decrease in the shrinkage ratio owing to the arrangement of the crack(s), the deformation behavior of coke models with the inert component and one crack is displayed in **Fig. 13**. In each condition, the coke matrix was deformed toward the inside of the analytical object at the position of the crack, and the crack was opened. Kubota *et al.*[13] showed theoretically that tensile stress occurred around an inert component. Our results also indicated that the crack was opened owing to the tensile stress. Furthermore, when the coke matrix was an elastic body and the elastic modulus of the inert component was 10 GPa, crack was deformed significantly. This should be because a high thermal stress occurred when the matrix was an elastic body and the elastic modulus of the inert component was large. Consequently, in the case of coke with an inert component, the shrinkage ratio of the coke should decrease because cracks were generated in the vicinity of the inert component, and these cracks were opened.

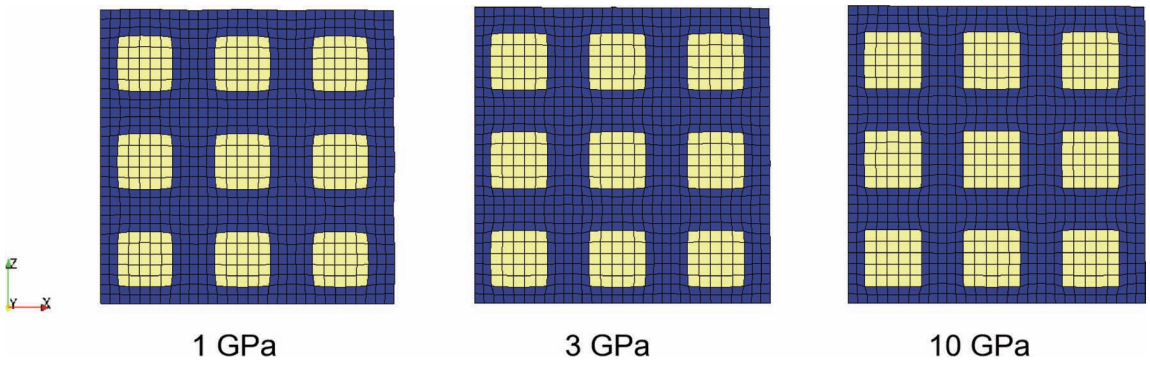

(a-1) Material arrangement. Blue-colored parts are coke matrices, and red-colored parts represent inert components in computational domain. (Matrix is assumed to be elastic.)

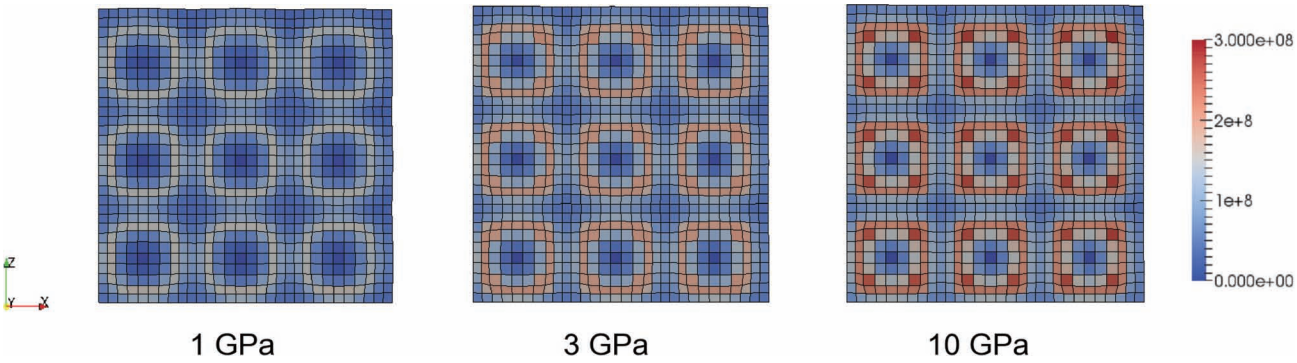

(a-2) von Mises stress distribution. (Matrix is assumed to be elastic.)

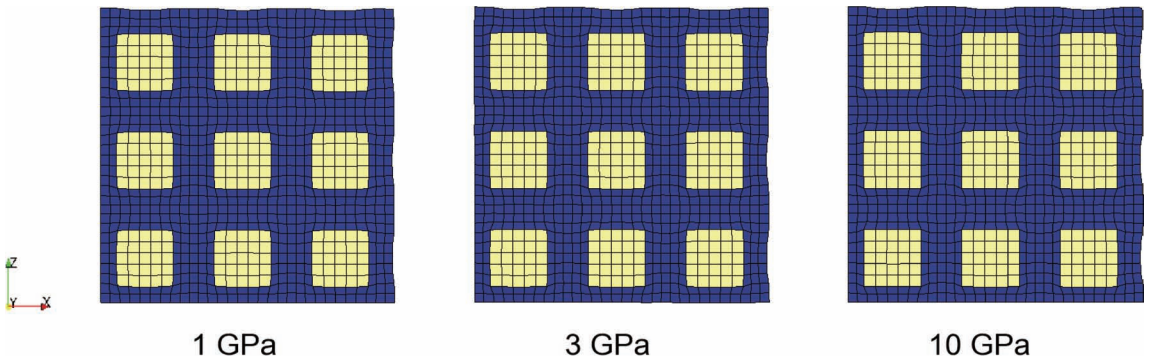

(b-1) Material arrangement. Blue-colored parts are coke matrices, and red-colored parts represent inert components in computational domain. (Matrix is assumed to be visco-elastic.)

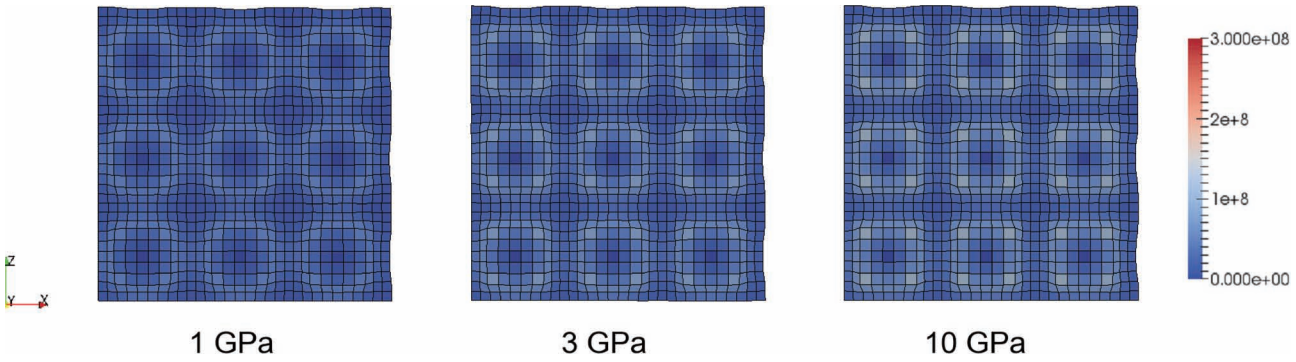

(b-2) von Mises stress distribution. (Matrix is assumed to be visco-elastic.)

Fig. 11. Deformed coke and von Mises stress distribution of coke model with coke matrix and small inert components in direction of y = 7.5 mm and temperature of 1 000°C with various elastic moduli of inert component. (Online version in color.)

Next, the effect of the number of cracks is discussed. In Fig. 12, the shrinkage ratio with the arrangement of three cracks drastically decreased compared to that with one crack. This is thought to be because the volume of void space caused by the crack opening increased with an increase in the total surface of the cracks. Fukada *et al.*[12] observed that the shrink-

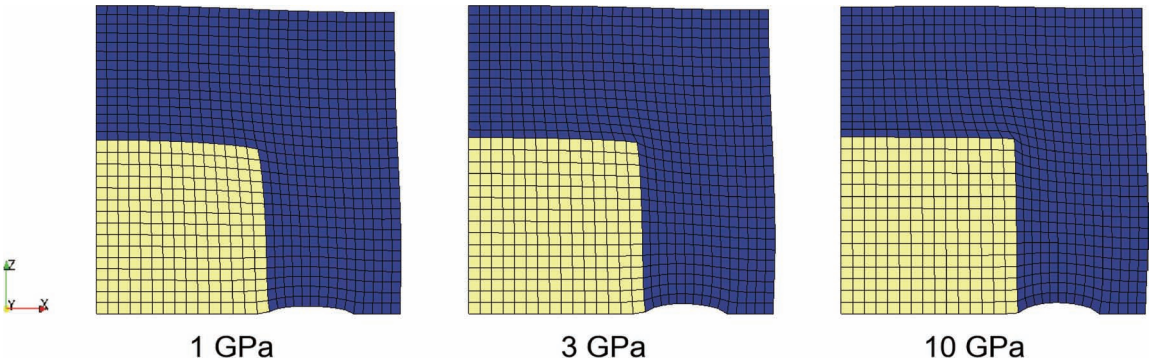

(a-1) Material arrangement. Blue-colored parts are coke matrices, and red-colored parts represent inert components in computational domain. (Matrix is assumed to be elastic.)

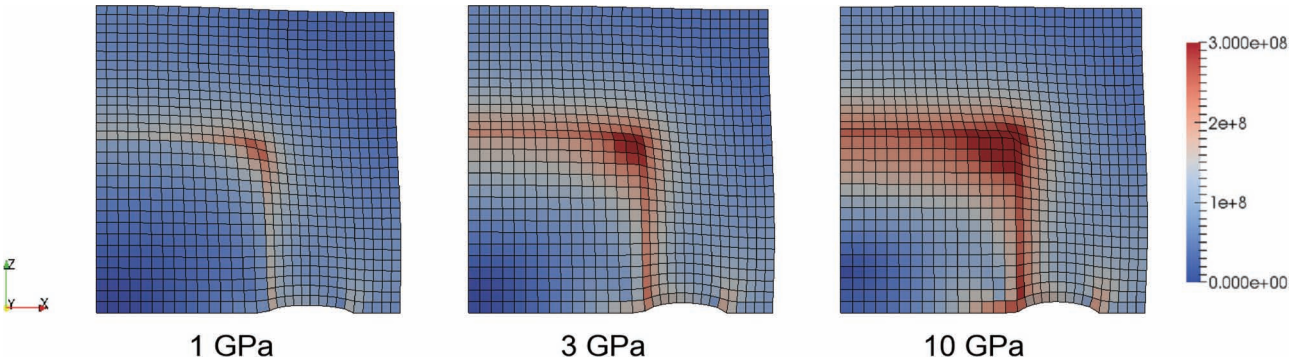

(a-2) von Mises stress distribution. (Matrix is assumed to be elastic.)

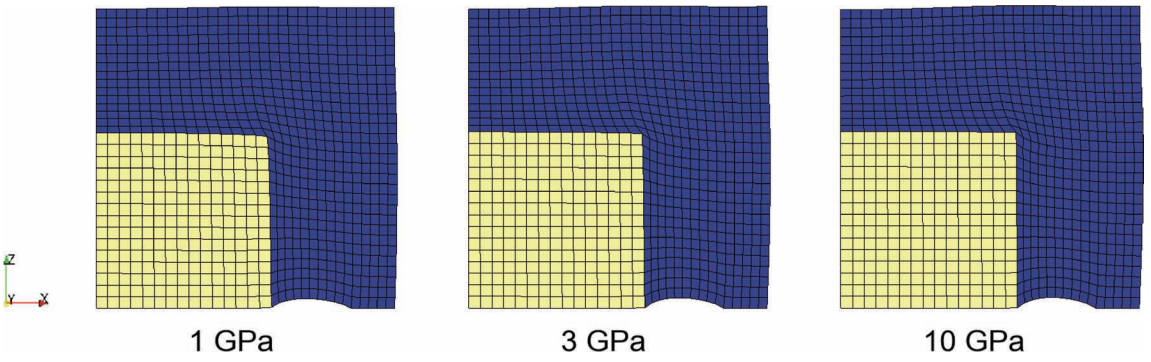

(b-1) Material arrangement. Blue-colored parts are coke matrices, and red-colored parts represent inert components in computational domain. (Matrix is assumed to be visco-elastic.)

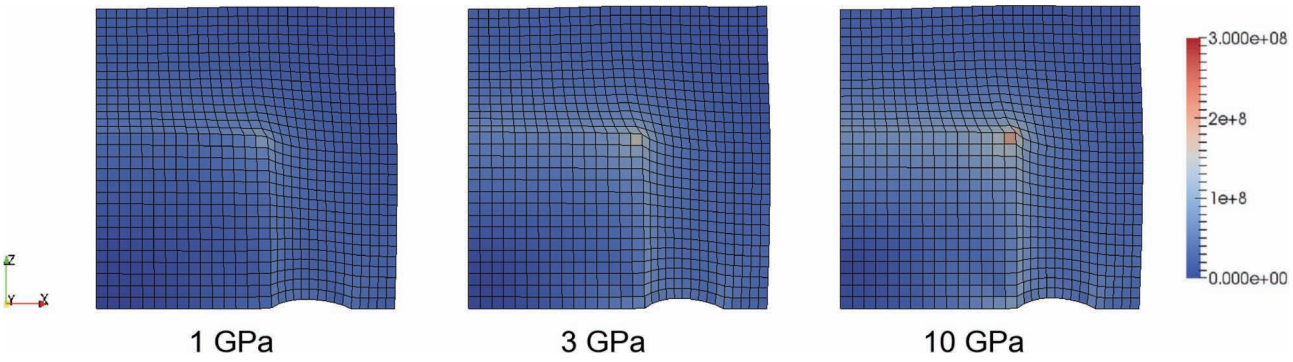

(b-2) von Mises stress distribution. (Matrix is assumed to be visco-elastic.)

Fig. 13. Deformed coke and von Mises stress distribution of coke model with coke matrix, one crack, and inert component in direction of y = 0 mm and temperature of 1 000°C with various elastic moduli of inert component. (Online version in color.)

age ratio of coke decreased with an increase in the number of cracks when inert components were added. Therefore, in the case of actual coke, the shrinkage ratio should be related to the number of cracks generated around the inert component. From the above results, it is suggested that the shrinkage ratio of coke decreased with an increase in the

number of cracks generated around the inert components.

4. Conclusion

In the present study, we performed a thermal stress analysis using the finite element method and investigated factors that affected the shrinkage ratio of coke, especially when an inert component was added. When an inert component with a large elastic modulus was added to coke, the contraction of coke was restricted. This should occur because the inert component with a large elastic modulus inhibited the shrinkage of the matrix, and the shrinkage ratio of the entire sample of semi-coke decreased. Moreover, when the semi-coke matrix showed viscous behavior, the matrix was deformable, and the shrinkage ratio increased. When the size of the inert component with a large elastic modulus was decreased, the contraction was restricted because of the increase in the area of the interface between the matrix and the inert component. Furthermore, cracks around the inert component decreased the shrinkage ratio significantly. This should be due to opening of cracks. In conclusion, we theoretically clarified the mechanism of the decrease in the shrinkage ratio of coke when inert components were added.

Acknowledgements

This work has been done in Research Group of Technique Elements for New Cokemaking Process in ISIJ (The chief examiner: Prof. H. Aoki, Tohoku Univ.). The authors would like to acknowledge the research group members gratefully.

Nomenclature

$\mathbf{B}$: B matrix
$\mathbf{D}$: elasticity matrix
$\mathbf{D}_T$: tangential stiffness matrix
d: nodal displacement [m]
f: nodal force [N]
G: shear modulus [Pa]
K: bulk modulus [Pa]
T: temperature [K]
t: time [s]

Greek symbols

α: shrinkage ratio [–]
Δ: increment
ε: strain [–]
λ: relaxation time [s]
σ: stress [Pa]
Ω: domain

Subscripts

d: deviatoric
n: time level

Superscripts

e: elastic
th: thermal

REFERENCES

1) T. Arima: *Tetsu-to-Hagané*, **92** (2006), 106 (in Japanese).
2) S. Nomura and T. Arima: *Fuel*, **105** (2013), 176.
3) D. R. Jenkins, M. R. Mahoney and J. C. Keating: *Fuel*, **89** (2010), 1654.
4) D. R. Jenkins and M. R. Mahoney: *Fuel*, **89** (2010), 1663.
5) D. R. Jenkins, D. E. Shaw and M. R. Mahoney: *Fuel*, **89** (2010), 1675.
6) M. D. Casal, E. Díaz-Faes, R. Alvarez, M. A. Díez and C. Barriocanal: *Fuel*, **85** (2006), 281.
7) M. Mahoney, S. Nomura, K. Fukuda, K. Kato, A. Le Bas, D. R. Jenkins and S. McGuire: *Fuel*, **89** (2010), 1557.
8) D. Merrick: *Fuel*, **62** (1983), 547.
9) S. Nomura and T. Arima: *Fuel*, **79** (2000), 1603.
10) R. Alvarez, J. J. Pis, M. A. Diez, A. Marzec and S. Czajkowska: *Energy Fuel.*, **11** (1997), 978.
11) A. Iwamoto, S. Matsuo, Y. Miyamoto, Y. Saito, Y. Matsushita, H. Aoki, Y. Kubota and H. Hayashizaki: *J. Jpn. Inst. Energy*, **97** (2018), 40.
12) K. Fukada, T. Yamamoto, I. Shimoyama, T. Anyashiki, H. Fujimoto and H. Sumi: *Tetsu-to-Hagané*, **93** (2007), 438 (in Japanese).
13) Y. Kubota, S. Nomura, T. Arima and K. Kato: *ISIJ Int.*, **48** (2008), 563.
14) Y. Kubota, K. Ikeda, T. Arima, S. Nomura and Y. Aihara: *Tetsu-to-Hagané*, **99** (2013), 175 (in Japanese).
15) R. Roest, H. Lomas, K. Hockings and M. R. Mahoney: *Fuel*, **180** (2016), 785.
16) R. Roest, H. Lomas and M. R. Mahoney: *Fuel*, **180** (2016), 794.
17) R. Roest, H. Lomas, S. Gupta, R. Kanniala and M. R. Mahoney: *Fuel*, **180** (2016), 803.
18) K. M. Steel, R. E. Dawson, D. R. Jenkins, R. Pearce and M. R. Mahoney: *Fuel Process. Technol.*, **155** (2017), 106.
19) K. Nushiro, T. Matsui, K. Hanaoka, K. Igawa and K. Sorimachi: *Tetsu-to-Hagané*, **81** (1995), 625 (in Japanese).
20) K. Hiraki, Y. Yamazaki, T. Kanai, A. Uchida, Y. Saito, Y. Matsushita, H. Aoki, T. Miura, S. Nomura and H. Hayashizaki: *ISIJ Int.*, **52** (2012), 1966.
21) N. Tsafnat, G. Tsafnat and A. S. Jones: *Miner. Eng.*, **22** (2009), 149.
22) N. Tsafnat, N. Amanat and A. S. Jones: *Fuel*, **90** (2011), 384.
23) A. Uchida, Y. Yamazaki, S. Matsuo, Y. Saito, Y. Matsushita, H. Aoki and M. Hamaguchi: *ISIJ Int.*, **56** (2016), 2132.
24) K. Ueoka, T. Ogata, Y. Matsushita, Y. Morozumi, H. Aoki, T. Miura, K. Uebo and K. Fukuda: *ISIJ Int.*, **47** (2007), 1723.
25) H. Sato, H. Aoki, T. Miura and J. W. Patrick: *Fuel*, **76** (1997), 311.
26) T. Ogata, K. Ueoka, Y. Morozumi, H. Aoki, T. Miura, K. Uebo and K. Fukuda: *Tetsu-to-Hagané*, **92** (2006), 171 (in Japanese).
27) O. C. Zienkiewicz, R. L. Taylor and D. D. Fox: The Finite Element Method for Solid and Structural Mechanics, 7th ed., Butterworth-Heinemann, Oxford, (2013), 77.